iScience

CellPress
OPEN ACCESS

Article

Follistatin controls the number of murine teeth by limiting TGF-β signaling

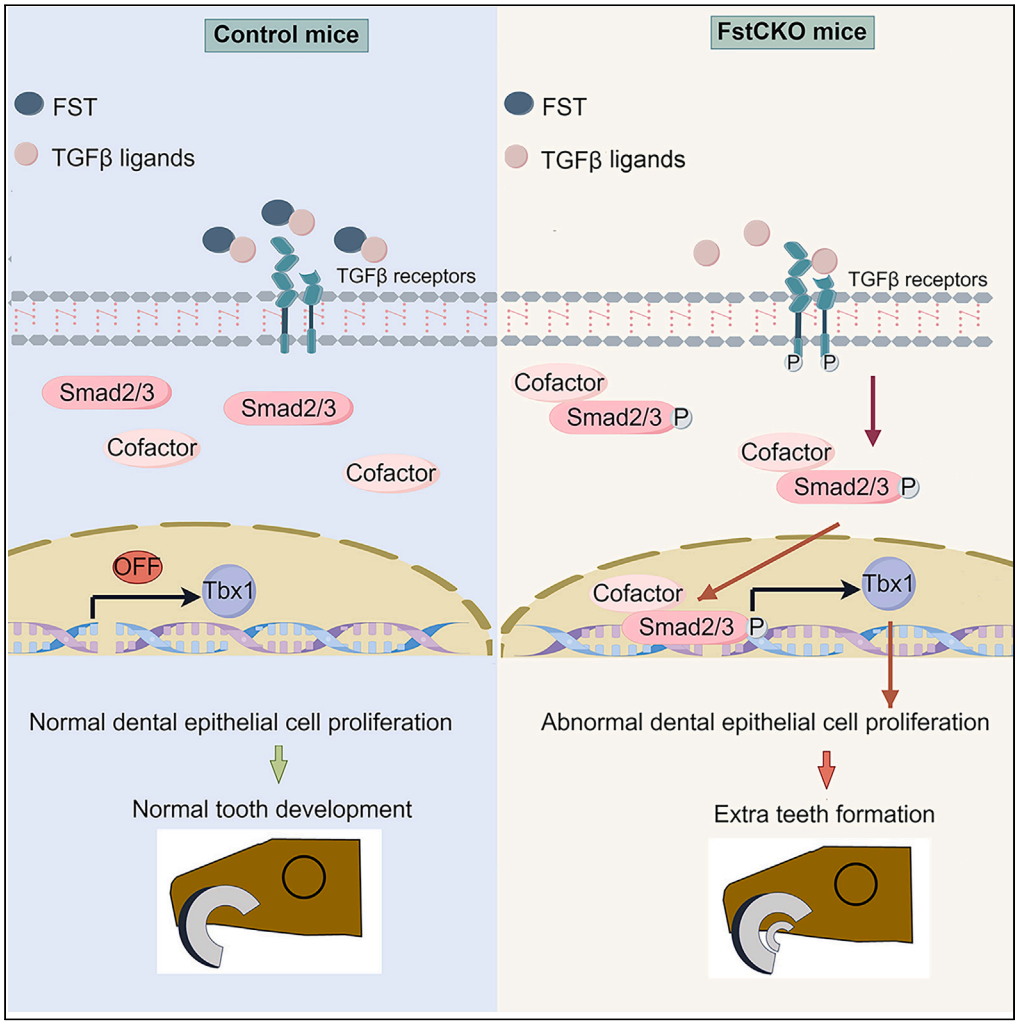

Shicheng Zhu, Suman Huo, Zhongzheng Wang, ..., Cheng Ding, Mengsheng Qiu, Xiao-Jing Zhu

xiao_jingzhu@hznu.edu.cn

Highlights

Conditional knockout of *Fst* leads to supernumerary upper incisor teeth in mice

Fst-deficiency activates TGF-β signaling and leads to increased cell proliferation

Tbx1, *Sp6*, and *Sox2* are identified as direct targets of TGF-β/SMAD2 signaling

Upregulation of *Tbx1* contributes to the formation of extra teeth in Fst^{CKO}

Zhu et al., iScience *27*, 110785
September 20, 2024
https://doi.org/10.1016/j.isci.2024.110785

iScience

CellPress
OPEN ACCESS

Article

Follistatin controls the number of murine teeth by limiting TGF-β signaling

Shicheng Zhu,[1,3] Suman Huo,[1,3] Zhongzheng Wang,[1,3] Caiyan Huang,[1] Chuanxu Li,[1] Hanjing Song,[1] Xueqin Yang,[1] Rui He,[2] Cheng Ding,[2] Mengsheng Qiu,[1] and Xiao-Jing Zhu[1,4,*]

SUMMARY

Supernumerary teeth are common developmental anomalies of dentition. However, the factors and mechanisms driving their formation remain largely unknown. Here, we report that conditional knockout of *Fst*, encoding an antagonist for the transforming growth factor β (TGF-β) signaling pathway, in both oral epithelium and mesenchyme of mice (*Fst*^{CKO}) led to supernumerary upper incisor teeth, arising from the lingual dental epithelium of the native teeth and preceded by an enlarged and split lingual cervical loop. *Fst*-deficiency greatly activated TGF-β signaling in developing maxillary incisor teeth, associated with increased epithelium cell proliferation. Moreover, *Fst*^{CKO} teeth exhibited increased expression of *Tbx1*, *Sp6*, and *Sox2*, which were identified as direct targets of TGF-β/SMAD2 signaling. Finally, we show that upregulation of *Tbx1* in response to *Fst*-deficiency was largely responsible for the formation of extra teeth in *Fst*^{CKO} mice. Taken together, our investigation indicates a novel role for *Fst* in controlling murine tooth number by restricting TGF-β signaling.

INTRODUCTION

Supernumerary teeth, defined as teeth that exceed the normal dental formula, are common dental anomalies in humans. Supernumerary teeth can manifest as a single tooth or multiple teeth, in a unilateral or bilateral fashion, and in any region of the dentition.[1,2] The most frequent site for an extra tooth is the anterior maxillary region. Supernumerary teeth can occur sporadically or are associated with syndromic diseases, such as amelogenesis imperfecta, Bloch-Sulzberger syndrome, craniosynostosis, cleidocranial dysplasia, and familial adenomatous polyposis.[1,2] The etiologies of tooth number abnormality are associated with the mechanisms that regulate tooth development, which have been extensively investigated using mouse models.[2] However, due to the variety and complexity of supernumerary tooth formation, more studies are required to explore the underlying mechanism.

Mammalian tooth development is tightly regulated by sequential and reciprocal interactions between the oral epithelium and the underlying cranial neural crest-derived mesenchyme. These interactions are mediated by multiple signaling pathways, including the wingless/integrated (WNT), bone morphogenetic protein (BMP), sonic hedgehog (SHH), and fibroblast growth factor (FGF) pathways.[3] Genetic disruption of these pathways often leads to dental anomalies, including the formation of supernumerary teeth.[2] β-Catenin is the core component of the Wnt signaling pathway. Mesenchymal ablation of β-catenin results in the formation of double incisors in mice,[4] whereas constitutive activation of β-catenin or conditional deletion of *Apc*, an inhibitor of canonical Wnt signaling, in the oral and dental epithelium leads to the formation of supernumerary teeth.[5,6] *Sostdc1* (ectodin, *USAG-1*, *Wise*) is a secreted inhibitor of WNT and BMP pathways. *Sostdc1*-deficient mice display one extra tooth bud that develops from the lingual dental epithelium of the mandible incisor.[7] It has been suggested that enhanced BMP signaling can account for supernumerary tooth formation in *Sostdc1* knockout mice.[8] Ectopic/expanded epithelial expression of *Shh* has been found in many mouse models with excess teeth.[4,5,7,9] Deletion of *Gas1*, which encodes an SHH antagonist in diastema mesenchyme, causes ectopic diastema teeth accompanied by increased SHH signaling activity.[10] The sprouty genes, which encode intracellular antagonists of FGF signaling, also play an essential role in regulating tooth number in mice.[9,11] One plausible explanation for supernumerary tooth formation is the revitalization of replacement teeth.[7]

Follistatin (FST) is an extracellular glycoprotein that binds to various ligands of the transforming growth factor β (TGF-β) superfamily, such as activins and BMPs, to limit their signaling potential. *Fst* knockout mice die within hours of birth, displaying developmental defects in the whiskers, teeth and muscles, and skeletal defects of the hard palate and the thirteenth pair of ribs.[12] Mouse incisor growth is fine-tuned by a balance between tooth wear and growth, which is underpinned by the renewal and differentiation of stem cells in both epithelial and mesenchymal stem cell niches.[13] The epithelial stem cells that give rise to enamel-producing ameloblasts are resident in a niche called the labial

[1]College of Life and Environmental Sciences, Zhejiang Key Laboratory of Organ Development and Regeneration, Hangzhou Normal University, Hangzhou, Zhejiang 311121, China
[2]The Affiliated Hospital, Hangzhou Normal University, Hangzhou, Zhejiang 310015, China
[3]These authors contributed equally
[4]Lead contact
*Correspondence: xiao_jingzhu@hznu.edu.cn
https://doi.org/10.1016/j.isci.2024.110785

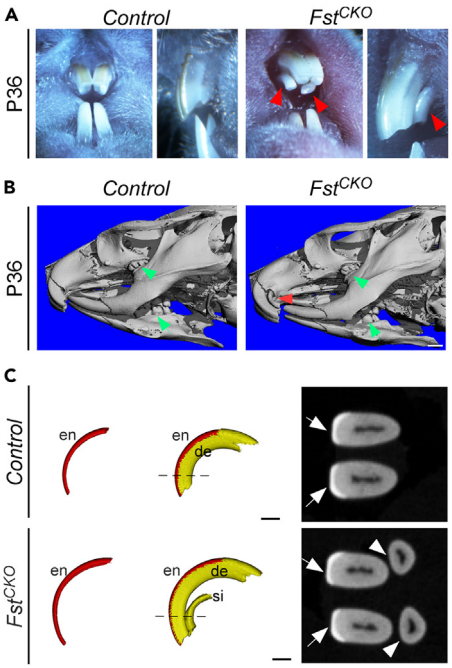

Figure 1. *Fst*-deficiency leads to extra maxillary incisors in mice

(A) Control mice display normal upper incisors. In contrast, Fst^{CKO} mice exhibit two extra maxillary incisors (arrowheads).

(B) Micro-CT reconstructions of skulls from P36 control and Fst^{CKO} mice. Molars are indicated by green arrows. Extra upper incisors in Fst^{CKO} mice are indicated by a red arrowhead.

(C) The left and the middle panels are three-dimensional images of micro-CT for upper incisors. The right panels are transverse micro-CT sections. The dashed lines represent the position of the right panel sections in the incisor. Enamel is indicated by arrows. Note the absence of enamel in the extra upper incisors of Fst^{CKO} mice (arrowheads). En, enamel; de, dentin; si, supernumerary incisor. Scale bars: 1 mm.

cervical loop (laCL) at the proximal end of the incisor. The other epithelial stem cells, which do not generate ameloblasts, are fewer and are located on the lingual side (liCL). In conventional *Fst* knockout mice, the liCL is enlarged and ameloblasts differentiate ectopically on the lingual surface, while epithelial *Fst* overexpression leads to severely hypoplastic cervical loops followed by inhibited ameloblast differentiation and loss of the enamel layer.[14]

To further decipher the regulatory mechanism of FST in tooth development, we created a mouse model (Fst^{CKO}) in which *Fst* is simultaneously knocked out in oral and dental epithelium and in the underlying mesenchyme. Intriguingly, we found that Fst^{CKO} mice displayed enamel-free supernumerary maxillary incisors. In addition, *Fst* is required to limit dental TGF-β signaling activity and to regulate the expression of a variety of genes essential for tooth development. *Fst*-deficiency also led to increased cell proliferation in upper teeth. Furthermore, we showed that several key genes in incisor development, including *Tbx1*, *Sp6*, and *Sox2*, are probably direct targets of TGF-β signaling. Finally, we demonstrated that upregulation of *Tbx1* in response to *Fst*-deficiency contributed to the generation of extra teeth in Fst^{CKO} mice.

RESULTS

Lack of *Fst* expression results in supernumerary upper incisor formation

Fst null mutant mice die shortly after birth[12]; therefore, we used conditional knockout mice of *Fst* to investigate the consequence of *Fst*-deficiency in postnatal development with a homozygous Fst^{Flox} allele.[15] *Fst* is expressed in the oral and dental epithelium and mesenchyme of all the tooth germs since E11.5.[14,16,17] To enable conditional inactivation of *Fst*, we generated homozygous Fst^{Flox} mice carrying the *K14-Cre* transgenic allele or *Wnt1-Cre* allele to delete *Fst* in oral and dental epithelium or in the underlying mesenchyme. However, *Fst* knockout mice driven by either Cre did not display defective tooth development (Figure S1). As FST is a secreted protein, it is possible that FST from the adjacent tissue can compensate for the FST-deficiency in the knockout tissue. Thus, we generated homozygous Fst^{Flox} mice carrying both *K14-Cre* and *Wnt1-Cre* (Fst^{CKO}) to enable deletion of *Fst* from both epithelium and the underlying mesenchyme of the developing teeth (Figures 1 and 2). Morphological observation revealed that control mice exhibited two maxillary incisors (Figure 1A, the left panels). Remarkably, Fst^{CKO} mice displayed supernumerary incisors adjacent to the native upper incisors on the lingual side (Figure 1A, the right panels; Figures S1B and S2C). Three-dimensional reconstruction of micro-computed tomography (CT) images of mouse skull also demonstrated the presence of extra upper incisors in Fst^{CKO} mice (Figure 1B). Micro-CT analysis further revealed that the extra incisors in Fst^{CKO} were enamel-free (Figure 1C, arrowheads). The native upper incisors of both control and Fst^{CKO} mice exhibited normal enamel deposition (Figure 1C, arrows). Among all the postnatal mice observed, the native upper incisors developed normally ($n > 10$). Lower incisors and molars also developed normally in Fst^{CKO} (Figure S3).

To investigate the timing of the first appearance of excess maxillary incisors, we examined histological sections from control and *Fst*-deficient mice during tooth development. A clear sign of supernumerary upper incisor formation in Fst^{CKO} mice was observed at E14.5 as a lingual enlargement and branching of the native tooth germ, which became more obvious at E16.5 (Figure 2A, arrows). At P10, the native upper incisors displayed normal enamel formation in both control and Fst^{CKO} mice (Figure 2B, the upper panels). By contrast, enamel was absent in the

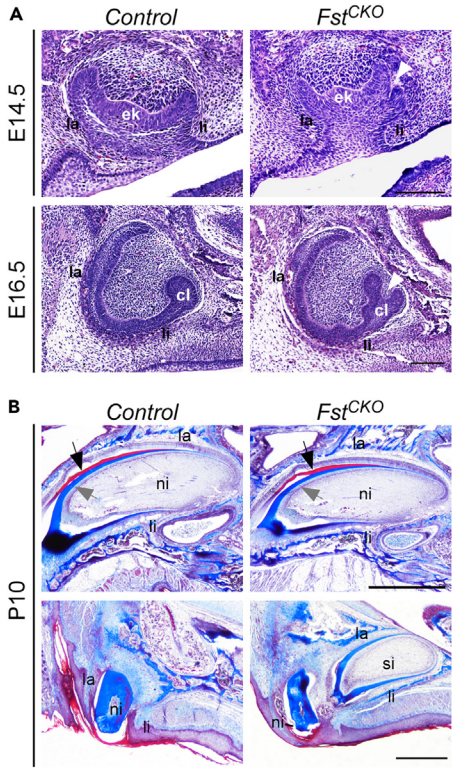

Figure 2. Histological analyses of upper incisor sagittal sections from control and Fst^{CKO} mice

(A) HE staining of upper incisor sagittal sections from control and Fst^{CKO} mice at E14.5 and E16.5. The liCL is enlarged and splits in Fst^{CKO} mice (arrows).
(B) Masson's trichrome staining showing normal native incisor development in control and Fst^{CKO} mice at P10 (the upper panels). Excess incisors are obvious in *Fst*-deficient mice at P10 (the lower right panel). Cl, cervical loop; ek, enamel knot; la, labial; li, lingual; ni, native incisor; si, supernumerary incisor. Scale bars: (A), 100 μm; (B), 500 μm.

extra teeth in Fst^{CKO} mice at P10 (Figure 2B, the right lower panel). Postnatal Fst^{CKO} mice, of both sexes, developed supernumerary incisor teeth with 100% penetration ($n > 10$). Additionally, all Fst^{CKO} embryos examined show sign of supernumerary upper incisor teeth ($n > 30$). Taken together, these results showed that loss of *Fst* leads to generation of enamel-free supernumerary upper incisors in mice.

Fst deficiency activates TGF-β signaling, upregulates SOX2 level, and leads to increased cell proliferation in the maxillary incisor

FST is an endogenous blocker of the TGF-β signaling pathway by neutralizing its ligands, such as activin.[18] We, therefore, first investigated the effect of *Fst*-deficiency on activin signaling in developing upper incisors at E14.5. Immunohistochemical staining of maxillary incisor sections showed that phosphorylated SMAD2 (*p*-SMAD2) was barely detected in the control mice. By contrast, positive *p*-SMAD2 immunoreactivity was observed throughout the upper incisor tooth germ, the adjacent mesenchyme, and oral epithelium in Fst^{CKO} mice (Figure 3A, the upper panel; Figure 3B), indicating that activin signaling was significantly increased in response to *Fst*-deficiency.

SOX2 plays essential roles in the maintenance of stem cell pluripotency and is required for dental stem cell proliferation and incisor development in mice.[13] SOX2 was expressed in the laCL of both control and Fst^{CKO} incisors at E14.5 (Figure 3A, the lower panel, arrowheads). In control incisors, SOX2 immunoreactivity was also found in the lingual dental and oral epithelium. Notably, increased and expanded SOX2 expression was found in the presumptive location of supernumerary teeth in *Fst*-deficient mice (Figure 3A, the lower panel, arrow), indicating the ectopic generation of epithelium stem cells for extra tooth formation in Fst^{CKO} mice.

Next, we investigated whether cell proliferation was altered in developing Fst^{CKO} upper incisors. We found that the number of cyclin D1-positive cells was significantly increased in the lingual dental epithelium of upper incisors deficient in *Fst* at E14.5 and E16.5 (Figures 3C and 3D). These observations demonstrated that *Fst* suppresses the proliferation of lingual dental epithelial cells in normal upper incisor development.

Fst-deficiency results in aberrant expression of key tooth development genes

To further elucidate the mechanism underlying incisor development mediated by FST, we investigated gene expression in maxillary incisors of Fst^{CKO} and control mice at E14.0 by RNA sequencing (RNA-seq). We identified 551 differentially expressed genes (DEGs) in upper incisors

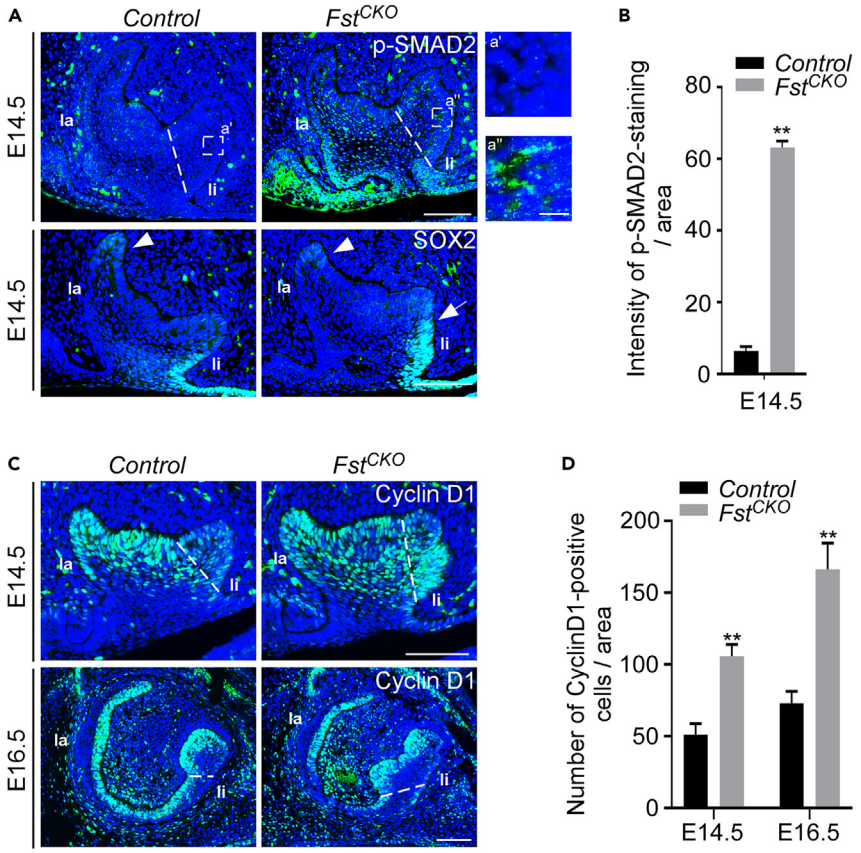

Figure 3. *Fst* deficiency activates TGF-β signaling, upregulates SOX2 level, and leads to increased cell proliferation in the maxillary incisor

(A) Immunofluorescence staining of sagittal sections showing increased *p*-SMAD2 and SOX2 levels in *Fst*-deficient upper incisors at E14.5. The magnified images of the regions within the dotted boxes (a' and a'') are shown to the right.

(B) Comparison of *p*-SMAD2 intensity in the designated areas of upper incisors in control and Fst^{CKO}.

(C) Immunofluorescence staining showing Cyclin D1 in sagittal sections of control and Fst^{CKO} upper incisors at E14.5 and E16.5.

(D) Statistical analysis revealing a significant increase in the number of cyclin D1-positive cells in the designated area of Fst^{CKO} upper incisors as compared with the control. The dental epithelium in the lingual side of the dashed line is used for analysis. Data are represented as mean ± SEM. ** Student's t test, $p < 0.01$. Scale bars, a' and a'', 50 μm; others, 100 μm.

between Fst^{CKO} and control mice (Table S1). As shown in the volcano plots, the expression of several key genes for tooth development, including *Osr1*, *Bmp3*, *Sp6*, *Tbx1*, *Irx1/2*, *Fgf15*, and *Odam*, was significantly changed in the mutant (Figure 4A). Among these genes, the expression of *Irx1* has been reported to be absent in all tooth germs of *activinβA* mutant embryos,[19] indicating that the TGF-β/activin signaling pathway is crucial for its expression. Therefore, the upregulation of *Irx1* in Fst^{CKO} teeth suggests that TGF-β/activin signaling activity is increased. Expression of several DEGs was validated by quantitative reverse transcription PCR (qRT-PCR) analysis (Figure 4B). Next, we performed enrichment analysis using Enrichr, a suite of gene set enrichment analysis tools,[20] with upregulated DEGs in Fst^{CKO}. Analysis against the "TF perturbations followed by expression table" revealed that the upregulated DEGs were mostly enriched with genes that were downregulated in *Smad3* knockout tissues (Figure S4). Given that activin signaling acts through SMAD2/3, this result also supports the notion that *Fst*-deficiency increases TGF-β signaling activity.

To further validate the RNA-seq data, we conducted *in situ* hybridization experiments involving *Sp6* and *Tbx1*. *Sp6* is essential for tooth development, as its absence leads to an overabundance of teeth, along with their malformed structures.[21] Conversely, transgenic mice exhibiting epithelial *Sp6*-overexpression develop fewer molars in the mandible.[22] *In situ* hybridization showed that *Sp6* transcripts were primarily located in the inner enamel epithelium (IEE) in both control and Fst^{CKO} upper incisors at E14.5; however, the area of *Sp6* expression was greatly expanded in Fst^{CKO} incisors (arrow, Figure 4C). At E16.5, *Sp6* was mainly expressed in the labial IEE and weakly expressed in the lingual IEE in control teeth (Figure 4C). In incisors lacking *Fst*, *Sp6* expression was detected in both the labial IEE and the branched IEE at the liCL (arrows, Figure 4C). *Tbx1* plays an important role in regulating incisor development. *Tbx1* knockout in mice leads to hypoplastic incisors lacking enamel.[23] *In situ* hybridization showed that *Tbx1* was mainly expressed in the dental epithelium near to the dental papilla mesenchyme in control upper incisors at E14.5 (Figure 4D). However, its expression in the lingual dental epithelium was significantly upregulated in Fst^{CKO} upper incisors (arrows, Figure 4D). At E16.5, *Tbx1* was mainly expressed in the inner dental epithelium on the labial side of the upper incisor

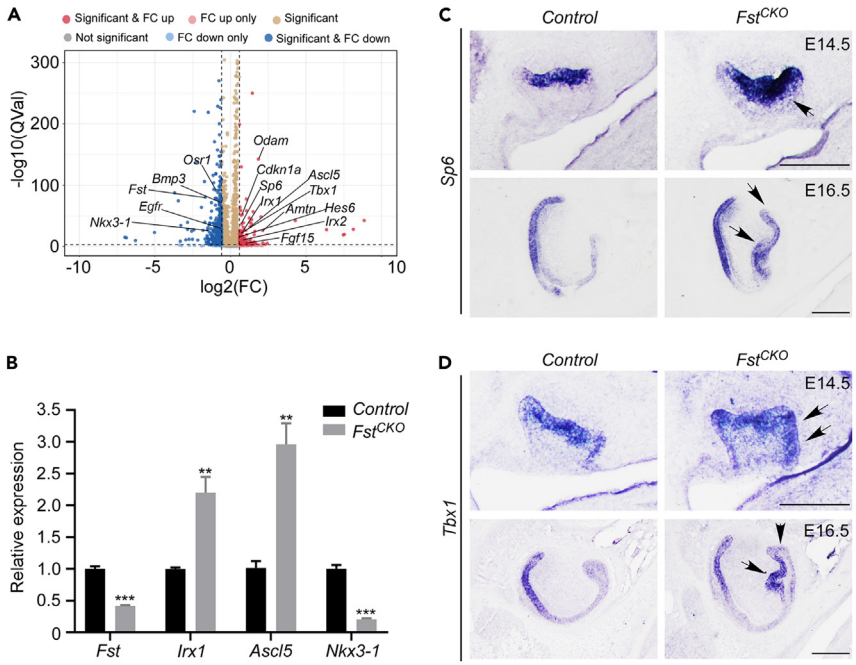

Figure 4. Differential gene expression in maxillary incisors lacking *Fst*

(A) Volcano plots of RNA-seq data showing gene expression differences between upper incisors from Fst^{CKO} mice and their control littermates at E14.0. Annotated dots indicate representative DEGs.

(B) Validation of RNA-seq data by qRT-PCR.

(C and D) *In situ* hybridization of sagittal sections showing the expression of *Sp6* and *Tbx1* in developing upper incisors. Ectopic and increased expression of *Sp6* and *Tbx1* in Fst^{CKO} upper incisors is marked by arrows. Data are represented as mean ± SEM. ** Student's t test, $p < 0.01$, *** Student's t test, $p < 0.001$. Scale bars, 200 μm.

and weakly expressed in the liCL (Figure 4D). In Fst^{CKO} mice, *Tbx1* transcript levels were greatly increased in the split liCL (arrows, Figure 4D). Overall, these results indicate that FST plays an important role in regulating the expression of key molecules for tooth development.

TGF-β signaling directly targets *Tbx1*, *Sp6*, and *Sox2* during tooth development

Due to the increased activity of the TGF-β signaling pathway resulting from the *Fst* knockout, we subsequently examined whether the crucial genes that are upregulated in Fst^{CKO} incisors are directly regulated by this pathway. Activation of activin/TGF-β signaling involves phosphorylation of SMAD2/3, which form heteromeric complexes with SMAD4. These then translocate to the nucleus and regulate target gene expression.[24] The presence of consensus *p*-SMAD2/3-binding sites, AGACWB,[25] were observed within regulatory regions of *Tbx1*, *Sp6*, *Sox2*, and *Ascl5* genome. We then used cleavage under targets and tagmentation (CUT&Tag) assays and *p*-SMAD2 antibody to examine whether these genes are TGF-β target genes in E14.0 upper incisor tooth samples. RT-PCR analysis of immunoprecipitated DNA showed that there was specific enrichment of *p*-SMAD2 to a DNA fragment that corresponds to one of potential sites from *Tbx1*, *Sp6*, and *Sox2* promoters with antibodies against *p*-SMAD2 (Figure 5A, arrows), suggesting that the expression of *Tbx1*, *Sp6*, and *Sox2* is probably directly regulated by TGF-β signaling in developing upper incisor. By contrast, the *p*-SMAD2 antibody did not enrich DNA fragments from the *Ascl5* promoter region (Figure 5A).

FST regulates the number of maxillary incisor teeth by upregulating *Tbx1*

Tbx1 plays critical roles in dental epithelial cell proliferation and its expression is upregulated in Fst^{CKO} incisors. Furthermore, *Tbx1* potentially contributes to the maintenance of epithelial stem cells through the regulation of *Sox2*.[26] Consequently, we investigated whether the upregulation of *Tbx1* is the primary driver behind the excessive teeth formation observed in Fst^{CKO} mice. Consistent with previous reports showing that *Tbx1* positively regulates cell proliferation,[23,27,28] our Cell Counting Kit 8 (CCK8) assay showed that knockdown of *TBX1* in HEK293T cells dramatically decreased cell proliferation (Figure 5B). Subsequently, we conducted a rescue experiment using organ culture to investigate whether the downregulation of *Tbx1* expression could potentially reverse the supernumerary tooth formation observed in *Fst*-deficient incisor teeth. Maxillary incisors were dissected, transfected with indicated siRNAs, and cultured in a Trowell-type organ culture system. Knockdown of *Fst* caused supernumerary tooth formation in the tooth explants. In contrast, knockdown of *Tbx1* led to hypoplastic incisor development (Figure 5C). Notably, supernumerary tooth formation in *Fst*-knockdown incisor explants was significantly rescued by knockdown of *Tbx1* (Figure 5C). Taken together, these results indicate that overexpression of *Tbx1* caused by *Fst*-deficiency can account for supernumerary incisor

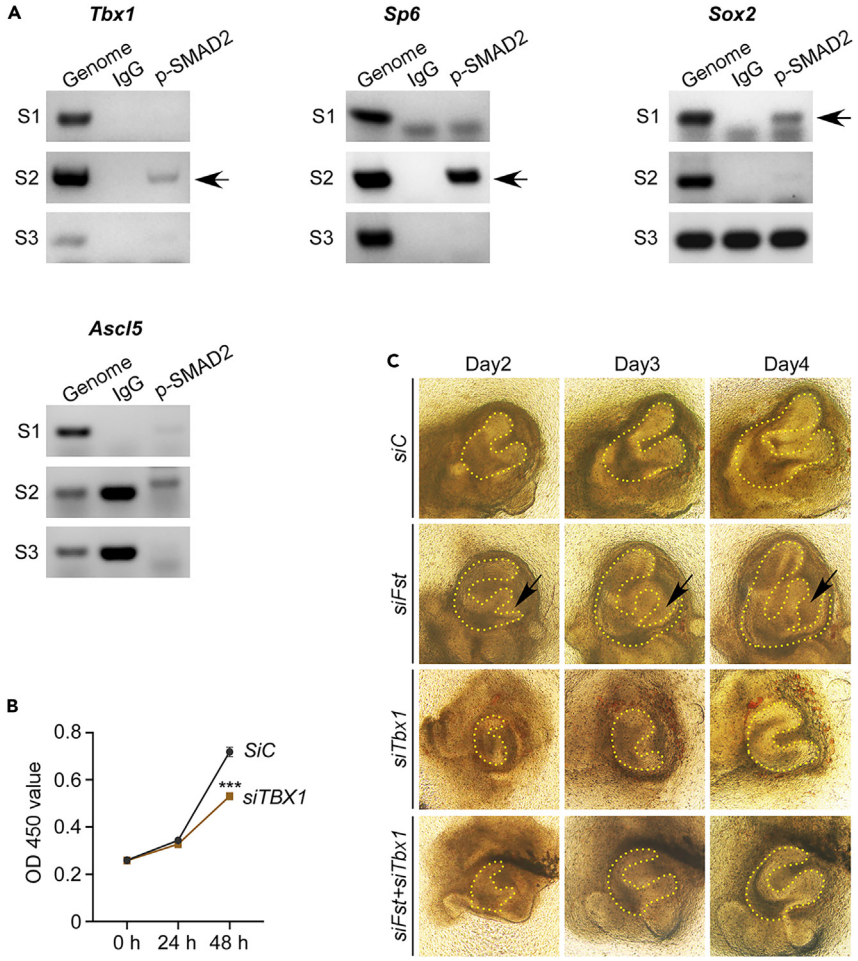

Figure 5. Activin/TGF-β signaling directly regulates key genes for incisor development and increased *Tbx1* expression accounts for supernumerary tooth formation in Fst^{CKO} mice

(A) CUT&Tag analysis showing the enrichment of DNA fragments containing *p*-SMAD2-binding sites (S1–3) in *Tbx1*, *Sp6*, and *Sox2*, but not in *Ascl5*. CUT&Tag analysis was performed with *p*-SMAD2 antibody and IgG control in mouse upper incisor tooth germs at around E14. Immunoprecipitated DNA was amplified by RT-PCR and analyzed by agarose gel electrophoresis. Fragments amplified using genomic DNA were used as positive controls for each primer set. Specific enrichment of *p*-SMAD2 to a DNA fragment containing potential *p*-SMAD2-binding sites is indicated by an arrow.

(B) CCK8 assay shows that knockdown of *TBX1* expression in HEK293T cells impairs cell proliferation.

(C) Rescue of *Fst*-deficiency-induced extra upper incisor formation by *Tbx1* knockdown in tooth explants. Maxillary incisors were dissected, transfected with indicated siRNAs, and cultured for 3 days after transfection. Data are represented as mean ± SEM. *** Student's t test, $p < 0.001$.

formation in Fst^{CKO} mice. Given that *Fst*-deficiency augments TGF-β signaling activity and *Tbx1* is the direct target of TGF-β signaling, these findings suggest that FST modulates tooth number through the regulation of TGF-β-mediated activation of *Tbx1*.

DISCUSSION

Supernumerary teeth are a common developmental anomaly of dentition. Here, we showed that *Fst* deficiency led to supernumerary upper incisor tooth formation in mice. The generation of extra teeth was associated with enhanced TGF-β signaling and increased cell proliferation. Furthermore, we showed that *Tbx1*, *Sp6*, and *Sox2* are probably direct targets of *p*-SMAD2 and that knockdown of *Tbx1* expression prevented extra tooth formation in *Fst*-deficient in tooth explants. Taken together, our investigation provides a novel mechanism at the cellular level for *Fst* controlling tooth number in mice.

Mouse incisors grow continuously throughout life because they have differential proximal niches that contain epithelial and mesenchymal stem cells respectively. *Fst* plays a critical role in regulating the proliferation of dental epithelial stem cells and transit amplifying cells.[17] Intriguingly, Fst^{CKO} mice exhibit supernumerary upper incisor tooth formation, rather than the generation of lingual enamel as in $Fst^{-/-}$ mice.[14] *Wnt1-Cre* line exhibits Cre recombination activity in cranial neural crest cell-derived mesenchymal cells at around E8.0.[29,30] *K14-Cre* becomes active in oral and dental epithelium from E11.5 and enables elimination of gene product at E12.5.[29] By that time, *Fst*

has already been deleted from all tissues of $Fst^{-/-}$. Therefore, it is possible that the timing of losing *Fst* controls the cell fate of dental epithelial stem cells, resulting in different phenotypes in Fst^{CKO} and $Fst^{-/-}$.

Moreover, unlike $Fst^{-/-}$ mice, native upper incisors of Fst^{CKO} mice are covered by enamel only on the labial side. The liCL of the *Fst*-deficient native incisor is split in two; therefore, it is reasonable that the remaining portion of the liCL has insufficient epithelial stem cells for producing enamel. Interestingly, the supernumerary upper incisors in Fst^{CKO} mice are enamel-free, which may also be caused by insufficient epithelial stem cells. Another possibility is that differentiation of the epithelial stem cells in the extra tooth is impaired.

$Fst^{-/-}$ mice exhibit an enlarged stem cell niche in the upper incisor. Excessive generation of SOX2-positive cells are present in Fst^{CKO} upper incisors, indicating that expansion of the CL area in $Fst^{-/-}$ teeth is probably associated with an increased number of SOX2-positive cells. These results, together with ectopic development of *Sox2*-expressing taste progenitors in the $Fst^{-/-}$ tongue,[31] support *Fst* as negatively regulating *Sox2* expression in various tissues. The small supernumerary teeth in Fst^{CKO} mice are located lingually to the native incisor, similar to the arrangement of rabbit upper incisor teeth. Studies in vertebrate with replacement tooth formation reveal the successional tooth forming on the lingual side of the deciduous tooth from the successional dental lamina, which displays *Sox2* expression.[32] In mice, a transient rudimentary successional dental lamina also forms and houses *Sox2*-positive cells.[32,33] Similarly, expanded SOX2 expression is observed in lingual dental epithelium of native upper incisors in Fst^{CKO} mice. Taken together, these results suggest that the formation of supernumerary teeth in Fst^{CKO} mice could be a result of revitalization of the rudimentary successional tooth germ.

TBX1 is the major genetic determinant of DiGeorge syndrome in humans. Mice deficient of *Tbx1* exhibit features of DiGeorge syndrome, including cardiac, craniofacial, and dental anomalies.[34] In mice, *Tbx1* plays a pivotal role in amelogenesis and in the maintenance of epithelial stem cells because *Tbx1* knockout leads to severely reduced or completely missing CL and hypoplastic and enamel-free incisors.[23] As in $Fst^{-/-}$mice, $Spry2^{+/-}$;$Spry4^{-/-}$ mutant lower incisors display enamel on both labial and lingual sides.[35] Loss of asymmetry in $Spry2^{+/-}$;$Spry4^{-/-}$ mice is associated with ectopically expressed *Tbx1* in the enlarged liCL.[23] *Tbx1* over-expression leads to increased laCL size and dental stem cell proliferation.[28] Together with the finding that *Tbx1* expression is increased in the liCL of Fst^{CKO} mice, these results indicate that the enlarged liCL of $Fst^{-/-}$ mice may also be associated with increased *Tbx1* expression in the liCL. We also showed that upregulation of *Tbx1* is required for extra teeth formation in Fst^{CKO} mice, which may also be attributed to its positive role in regulating epithelial stem cell proliferation. Intriguingly, it is reported that *Tbx1* possibly acts upstream of *Sox2*.[26] Together with the fact that *Sox2* is essential for epithelial stem cell proliferation and is upregulated in Fst^{CKO} incisor germs, these results indicate that *Tbx1* could regulate dental epithelial stem cell proliferation by regulating *Sox2*. However, more experiments are required to illustrate the regulatory relationship of *Tbx1* and *Sox2* in further studies.

In this report, we show that FST acts upstream of multiple key tooth development genes and is involved in determining tooth number. These findings, together with other advances in the molecular mechanisms underlying supernumerary tooth formation and in stem cell biology, will help reveal the etiology of supernumerary teeth in humans and will be informative for tooth regeneration and tooth engineering.

Limitations of the study

Our study shows that FST-deficiency leads to supernumerary incisor teeth in mice, suggesting that FST can be used as a novel target for tooth regeneration, however, more experiments should be conducted to prove this possibility in other animal models in future studies.

RESOURCE AVAILABILITY

Lead contact

Further information and requests for resources and reagents should be directed to the lead contact, Xiao-Jing Zhu (xiao_jingzhu@hznu.edu.cn).

Materials availability

This study did not generate new unique materials or reagents.

Data and code availability

- The RNA-seq data have been deposited in the Genome Sequence Archive of the National Genomics Data Center, China National Center for Bioinformation/Beijing Institute of Genomics, Chinese Academy of Sciences, and is publicly accessible as of the date of publication. Accession number is listed in the key resources table.
- This paper does not report original code.
- Any additional information required to reanalyze the data reported in this paper is available from the lead contact upon request.

ACKNOWLEDGMENTS

The authors thank Dr. Martin Matzuk from Baylor College of Medicine for kindly providing Fst^{CKO} mice for the study. We thank all members of the Zhang laboratory at Zhejiang Key Laboratory of Organ Development and Regeneration, Hangzhou Normal University for helpful discussions.

AUTHOR CONTRIBUTIONS

S.Z., S.H., and Z.W.: contributed to data acquisition, analysis, and interpretation and critically revised the manuscript. C.H., C.L., H.S., and X.Y.: contributed to data acquisition and analysis and critically revised the manuscript. R.H., C.D., and M.Q.: contributed to data analysis and critically revised the manuscript. X.J.Z.: contributed to design, data interpretation, drafted and critically revised the manuscript. All authors gave their final approval and agree to be accountable for all aspects of the work.

DECLARATION OF INTERESTS

The authors declare no competing interests.

STAR★METHODS

Detailed methods are provided in the online version of this paper and include the following:

- KEY RESOURCES TABLE
- EXPERIMENTAL MODEL AND STUDY PARTICIPANT DETAILS
  - Ethics statement
  - Animals
- METHOD DETAILS
  - MicroCT, histology, immunohistochemistry, and *in situ* hybridization
  - RNA-Seq
  - Quantitative reverse transcription PCR (qRT-PCR)
  - CUT&Tag
  - CCK8 assays
  - Organ culture
- QUANTIFICATION AND STATISTICAL ANALYSIS

SUPPLEMENTAL INFORMATION

Supplemental information can be found online at https://doi.org/10.1016/j.isci.2024.110785.

Received: April 24, 2024
Revised: June 24, 2024
Accepted: August 19, 2024
Published: August 22, 2024

REFERENCES

1. Lu, X., Yu, F., Liu, J., Cai, W., Zhao, Y., Zhao, S., and Liu, S. (2017). The epidemiology of supernumerary teeth and the associated molecular mechanism. Organogenesis *13*, 71–82. https://doi.org/10.1080/15476278.2017.1332554.
2. Zhang, H., Gong, X., Xu, X., Wang, X., and Sun, Y. (2023). Tooth number abnormality: from bench to bedside. Int. J. Oral Sci. *15*, 5. https://doi.org/10.1038/s41368-022-00208-x.
3. Hermans, F., Hemeryck, L., Lambrichts, I., Bronckaers, A., and Vankelecom, H. (2021). Intertwined Signaling Pathways Governing Tooth Development: A Give-and-Take Between Canonical Wnt and Shh. Front. Cell Dev. Biol. *9*, 758203. https://doi.org/10.3389/fcell.2021.758203.
4. Fujimori, S., Novak, H., Weissenbock, M., Jussila, M., Goncalves, A., Zeller, R., Galloway, J., Thesleff, I., and Hartmann, C. (2010). Wnt/beta-catenin signaling in the dental mesenchyme regulates incisor development by regulating Bmp4. Dev. Biol. *348*, 97–106. https://doi.org/10.1016/j.ydbio.2010.09.009.
5. Wang, X.P., O'Connell, D.J., Lund, J.J., Saadi, I., Kuraguchi, M., Turbe-Doan, A., Cavallesco, R., Kim, H., Park, P.J., Harada, H., et al. (2009). Apc inhibition of Wnt signaling regulates supernumerary tooth formation during embryogenesis and throughout adulthood. Development *136*, 1939–1949. https://doi.org/10.1242/dev.033803.
6. Järvinen, E., Salazar-Ciudad, I., Birchmeier, W., Taketo, M.M., Jernvall, J., and Thesleff, I. (2006). Continuous tooth generation in mouse is induced by activated epithelial Wnt/beta-catenin signaling. Proc. Natl. Acad. Sci. USA *103*, 18627–18632. https://doi.org/10.1073/pnas.0607289103.
7. Munne, P.M., Tummers, M., Järvinen, E., Thesleff, I., and Jernvall, J. (2009). Tinkering with the inductive mesenchyme: Sostdc1 uncovers the role of dental mesenchyme in limiting tooth induction. Development *136*, 393–402. https://doi.org/10.1242/dev.025064.
8. Murashima-Suginami, A., Takahashi, K., Sakata, T., Tsukamoto, H., Sugai, M., Yanagita, M., Shimizu, A., Sakurai, T., Slavkin, H.C., and Bessho, K. (2008). Enhanced BMP signaling results in supernumerary tooth formation in USAG-1 deficient mouse. Biochem. Biophys. Res. Commun. *369*, 1012–1016. https://doi.org/10.1016/j.bbrc.2008.02.135.
9. Klein, O.D., Minowada, G., Peterkova, R., Kangas, A., Yu, B.D., Lesot, H., Peterka, M., Jernvall, J., and Martin, G.R. (2006). Sprouty genes control diastema tooth development via bidirectional antagonism of epithelial-mesenchymal FGF signaling. Dev. Cell *11*, 181–190. https://doi.org/10.1016/j.devcel.2006.05.014.
10. Ohazama, A., Haycraft, C.J., Seppala, M., Blackburn, J., Ghafoor, S., Cobourne, M., Martinelli, D.C., Fan, C.M., Peterkova, R., Lesot, H., et al. (2009). Primary cilia regulate Shh activity in the control of molar tooth number. Development *136*, 897–903. https://doi.org/10.1242/dev.027979.
11. Charles, C., Hovorakova, M., Ahn, Y., Lyons, D.B., Marangoni, P., Churava, S., Biehs, B., Jheon, A., Lesot, H., Balooch, G., et al. (2011). Regulation of tooth number by fine-tuning levels of receptor-tyrosine kinase signaling. Development *138*, 4063–4073. https://doi.org/10.1242/dev.069195.
12. Matzuk, M.M., Lu, N., Vogel, H., Sellheyer, K., Roop, D.R., and Bradley, A. (1995). Multiple defects and perinatal death in mice deficient in follistatin. Nature *374*, 360–363. https://doi.org/10.1038/374360a0.
13. Sun, Z., Yu, W., Sanz Navarro, M., Sweat, M., Eliason, S., Sharp, T., Liu, H., Seidel, K., Zhang, L., Moreno, M., et al. (2016). Sox2 and Lef-1 interact with Pitx2 to regulate incisor development and stem cell renewal. Development *143*, 4115–4126. https://doi.org/10.1242/dev.138883.
14. Wang, X.P., Suomalainen, M., Jorgez, C.J., Matzuk, M.M., Werner, S., and Thesleff, I. (2004). Follistatin regulates enamel patterning in mouse incisors by asymmetrically inhibiting BMP signaling and ameloblast differentiation. Dev. Cell *7*, 719–730. https://doi.org/10.1016/j.devcel.2004.09.012.
15. Jorgez, C.J., Klysik, M., Jamin, S.P., Behringer, R.R., and Matzuk, M.M. (2004). Granulosa cell-specific inactivation of follistatin causes female fertility defects. Mol. Endocrinol. *18*, 953–967. https://doi.org/10.1210/me.2003-0301.
16. Ferguson, C.A., Tucker, A.S., Christensen, L., Lau, A.L., Matzuk, M.M., and Sharpe, P.T. (1998). Activin is an essential early mesenchymal signal in tooth development that is required for patterning of the murine dentition. Genes Dev. *12*, 2636–2649. https://doi.org/10.1101/gad.12.16.2636.
17. Wang, X.P., Suomalainen, M., Felszeghy, S., Zelarayan, L.C., Alonso, M.T., Plikus, M.V., Maas, R.L., Chuong, C.M., Schimmang, T., and Thesleff, I. (2007). An integrated gene regulatory network controls stem cell proliferation in teeth. PLoS Biol. *5*, e159. https://doi.org/10.1371/journal.pbio.0050159.
18. Prajapati-DiNubila, M., Benito-Gonzalez, A., Golden, E.J., Zhang, S., and Doetzlhofer, A. (2019). A counter gradient of Activin A and follistatin instructs the timing of hair cell differentiation in the murine cochlea. Elife *8*, e47613. https://doi.org/10.7554/eLife.47613.
19. Ferguson, C.A., Tucker, A.S., Heikinheimo, K., Nomura, M., Oh, P., Li, E., and Sharpe, P.T. (2001). The role of effectors of the activin signalling pathway, activin receptors IIA and

IIB, and Smad2, in patterning of tooth development. Development *128*, 4605–4613. https://doi.org/10.1242/dev.128.22.4605.

20. Xie, Z., Bailey, A., Kuleshov, M.V., Clarke, D.J.B., Evangelista, J.E., Jenkins, S.L., Lachmann, A., Wojciechowicz, M.L., Kropiwnicki, E., Jagodnik, K.M., et al. (2021). Gene Set Knowledge Discovery with Enrichr. Curr. Protoc. *1*, e90. https://doi.org/10.1002/cpz1.90.
21. Nakamura, T., de Vega, S., Fukumoto, S., Jimenez, L., Unda, F., and Yamada, Y. (2008). Transcription factor epiprofin is essential for tooth morphogenesis by regulating epithelial cell fate and tooth number. J. Biol. Chem. *283*, 4825–4833. https://doi.org/10.1074/jbc.M708388200.
22. Nakamura, T., Jimenez-Rojo, L., Koyama, E., Pacifici, M., de Vega, S., Iwamoto, M., Fukumoto, S., Unda, F., and Yamada, Y. (2017). Epiprofin Regulates Enamel Formation and Tooth Morphogenesis by Controlling Epithelial-Mesenchymal Interactions During Tooth Development. J. Bone Miner. Res. *32*, 601–610. https://doi.org/10.1002/jbmr.3024.
23. Catón, J., Luder, H.U., Zoupa, M., Bradman, M., Bluteau, G., Tucker, A.S., Klein, O., and Mitsiadis, T.A. (2009). Enamel-free teeth: Tbx1 deletion affects amelogenesis in rodent incisors. Dev. Biol. *328*, 493–505. https://doi.org/10.1016/j.ydbio.2009.02.014.
24. Li, S.N., and Wu, J.F. (2020). TGF-beta/SMAD signaling regulation of mesenchymal stem cells in adipocyte commitment. Stem Cell Res. Ther. *11*, 41. https://doi.org/10.1186/s13287-020-1552-y.
25. Liu, L., Liu, X., Ren, X., Tian, Y., Chen, Z., Xu, X., Du, Y., Jiang, C., Fang, Y., Liu, Z., et al. (2016). Smad2 and Smad3 have differential sensitivity in relaying TGFbeta signaling and inversely regulate early lineage specification. Sci. Rep. *6*, 21602. https://doi.org/10.1038/srep21602.
26. Gao, S., Li, X., and Amendt, B.A. (2013). Understanding the role of Tbx1 as a candidate gene for 22q11.2 deletion syndrome. Curr. Allergy Asthma Rep. *13*, 613–621. https://doi.org/10.1007/s11882-013-0384-6.
27. Cao, H., Florez, S., Amen, M., Huynh, T., Skobe, Z., Baldini, A., and Amendt, B.A. (2010). Tbx1 regulates progenitor cell proliferation in the dental epithelium by modulating Pitx2 activation of p21. Dev. Biol. *347*, 289–300. https://doi.org/10.1016/j.ydbio.2010.08.031.
28. Gao, S., Moreno, M., Eliason, S., Cao, H., Li, X., Yu, W., Bidlack, F.B., Margolis, H.C., Baldini, A., and Amendt, B.A. (2015). TBX1 protein interactions and microRNA-96-5p regulation controls cell proliferation during craniofacial and dental development: implications for 22q11.2 deletion syndrome. Hum. Mol. Genet. *24*, 2330–2348. https://doi.org/10.1093/hmg/ddu750.
29. Zhu, X., Zhao, P., Liu, Y., Zhang, X., Fu, J., Ivy Yu, H.M., Qiu, M., Chen, Y., Hsu, W., and Zhang, Z. (2013). Intra-epithelial requirement of canonical Wnt signaling for tooth morphogenesis. J. Biol. Chem. *288*, 12080–12089. https://doi.org/10.1074/jbc.M113.462473.
30. Liu, Y., Wang, M., Zhao, W., Yuan, X., Yang, X., Li, Y., Qiu, M., Zhu, X.J., and Zhang, Z. (2015). Gpr177-mediated Wnt Signaling Is Required for Secondary Palate Development. J. Dent. Res. *94*, 961–967. https://doi.org/10.1177/0022034515583532.
31. Beites, C.L., Hollenbeck, P.L.W., Kim, J., Lovell-Badge, R., Lander, A.D., and Calof, A.L. (2009). Follistatin modulates a BMP autoregulatory loop to control the size and patterning of sensory domains in the developing tongue. Development *136*, 2187–2197. https://doi.org/10.1242/dev.030544.
32. Juuri, E., Jussila, M., Seidel, K., Holmes, S., Wu, P., Richman, J., Heikinheimo, K., Chuong, C.M., Arnold, K., Hochedlinger, K., et al. (2013). Sox2 marks epithelial competence to generate teeth in mammals and reptiles. Development *140*, 1424–1432. https://doi.org/10.1242/dev.089599.
33. Popa, E.M., Buchtova, M., and Tucker, A.S. (2019). Revitalising the rudimentary replacement dentition in the mouse. Development *146*, dev171363. https://doi.org/10.1242/dev.171363.
34. Jerome, L.A., and Papaioannou, V.E. (2001). DiGeorge syndrome phenotype in mice mutant for the T-box gene, Tbx1. Nat. Genet. *27*, 286–291. https://doi.org/10.1038/85845.
35. Klein, O.D., Lyons, D.B., Balooch, G., Marshall, G.W., Basson, M.A., Peterka, M., Boran, T., Peterkova, R., and Martin, G.R. (2008). An FGF signaling loop sustains the generation of differentiated progeny from stem cells in mouse incisors. Development *135*, 377–385. https://doi.org/10.1242/dev.015081.
36. Zhu, X.J., Yuan, X., Wang, M., Fang, Y., Liu, Y., Zhang, X., Yang, X., Li, Y., Li, J., Li, F., et al. (2017). A Wnt/Notch/Pax7 signaling network supports tissue integrity in tongue development. J. Biol. Chem. *292*, 9409–9419. https://doi.org/10.1074/jbc.M117.789438.
37. Chen, E.Y., Tan, C.M., Kou, Y., Duan, Q., Wang, Z., Meirelles, G.V., Clark, N.R., and Ma'ayan, A. (2013). Enrichr: interactive and collaborative HTML5 gene list enrichment analysis tool. BMC Bioinf. *14*, 128. https://doi.org/10.1186/1471-2105-14-128.
38. Kuleshov, M.V., Jones, M.R., Rouillard, A.D., Fernandez, N.F., Duan, Q., Wang, Z., Koplev, S., Jenkins, S.L., Jagodnik, K.M., Lachmann, A., et al. (2016). Enrichr: a comprehensive gene set enrichment analysis web server 2016 update. Nucleic Acids Res. *44*, W90–W97. https://doi.org/10.1093/nar/gkw377.
39. Spandidos, A., Wang, X., Wang, H., and Seed, B. (2010). PrimerBank: a resource of human and mouse PCR primer pairs for gene expression detection and quantification. Nucleic Acids Res. *38*, D792–D799. https://doi.org/10.1093/nar/gkp1005.

STAR★METHODS

KEY RESOURCES TABLE

REAGENT or RESOURCE	SOURCE	IDENTIFIER
Antibodies		
phospho-SMAD2	Thermo Fisher Scientific	Cat#44-244G, RRID:AB_2533614
SOX2	Abcam	Cat#ab97959, RRID:AB_2341193
Cyclin D1	Abcam	Cat#ab134175, RRID:AB_2750906
Critical commercial assays		
Masson's Trichrome stain kit	Solarbio life sciences	Cat#G1340
RevertAid™ Master Mix	Thermo Fisher Scientific	Cat# M1632
UltraSYBR mixture	CWBIO	Cat#E606335
Trizol	Thermo Fisher Scientific	Cat# 15596026CN
T7 RNA polymerase	Promega	Cat# P2075
Sp6 RNA polymerase	Promega	Cat# P1085
DIG RNA Labeling Mix	Roche	Cat#11277073910
Anti-DIG-AP Fab fragments	Roche	Cat#11093274910
BM purple	Roche	Cat#11442074001
Hyperactive In-Situ ChIP Library Prep Kit for Illumina (pA-Tn5)	Vazyme	Cat#TD902
CCK8	Sangon	Cat#E606335
Lipofectamine® 3000	Thermo Fisher Scientific	Cat# L3000015
Deposited data		
RNA-Seq data of E14.0 upper incisors	This paper	GSA:CRA007363
Experimental models: Cell lines		
HEK293T	ATCC	Cat#CRL-3216
Experimental models: Organisms/strains		
Mouse: *Fst*$^{Flox/Flox}$	From Dr. Martin Matzuk	Jorgez et al.[15]
Mouse: *Wnt1-Cre*	The Jackson Laboratory	JAX: 004782
Mouse: *K14-Cre*	The Jackson Laboratory	JAX: 007807
Oligonucleotides		
Genotyping, QPCR and amplification primers for probe construction: see Table S2	This paper	N/A
RT-PCR primers: see Table S3	This paper	N/A
TBX1 siRNA: UGACCAAUAACCUGCUGGA	This paper	N/A
Tbx1 siRNA: UGACCAAUAACCUGCUGGA	This paper	N/A
Fst siRNA: GGAUGUGAACGACAAUACU	This paper	N/A
Recombinant DNA		
pGEM®-T Easy Vector	Promega	Cat#A1360
pGEM®-T-Fst	This paper	N/A
pGEM®-T-Sp6	This paper	N/A
pGEM®-T-Tbx1	This paper	N/A
Software and algorithms		
GraphPad Prism 9.5	Graphpad Software	http://www.graphpad.com/
Photoshop	Photoshop Software	https://www.adobe.com

EXPERIMENTAL MODEL AND STUDY PARTICIPANT DETAILS

Ethics statement

All animal experiments were approved by the Animal Users Committee of Hangzhou Normal University and carried out in strict accordance with the Guide for the Care and Use of Laboratory Animals at Hangzhou Normal University.

Animals

Fst$^{Flox/Flox}$ mice have been described previously.[15] *Wnt1-Cre* and *K14-Cre* mouse lines were purchased from The Jackson Laboratory (Bar Harbor, ME, USA). The mice are on the C57BL/6 background and were reared in specific pathogen free facilities. *Fst*$^{Flox/Flox}$ mice were crossed with the mice carrying both *Wnt1-Cre* and *K14-Cre* to obtain *Fst*$^{Flox/+;Wnt1\text{-}Cre;K14\text{-}Cre}$ mice, which were back-crossed with *Fst*$^{Flox/Flox}$ to produce *Fst*$^{Flox/Flox;Wnt1\text{-}Cre;K14\text{-}Cre}$ (*Fst*^{CKO}). *Fst*$^{Flox/Flox}$, and Cre^{-} or Cre^{+};*Fst*$^{Flox/+}$ littermates were used as control mice. Primer sequences for genotyping are shown in Table S2. The morning of vaginal plug appearance was determined as embryonic day 0.5. The experiment was conducted using mouse embryos at E14.0, E14.5, and E16.5, as well as postnatal mice at P0, P36, and four months of age. Gender does not affect the experimental results, as both female and male *Fst*^{CKO} mice exhibit the hyperdontia phenotype. All of the available *Fst*^{CKO} mice, both male and female, were arbitrarily used for experiments.

METHOD DETAILS

MicroCT, histology, immunohistochemistry, and *in situ* hybridization

For microCT analysis, post-natal day (P)36 mice were euthanized and dissected tissues were fixed in 4% paraformaldehyde and processed according to standard protocols. Embryos were dissected and fixed in 4% PFA (Sangon, Shanghai, China) overnight at 4°C. Samples were dehydrated through an ethanol series and embedded in paraffin. After deparaffinization and hydration, 7 μm sections were stained with hematoxylin and eosin (HE) following standard protocols. Masson trichrome staining was performed using a Masson's Trichrome stain kit (Solarbio life sciences, Beijing, China) according to the manufacturer's instructions. Standard hematoxylin/eosin (HE) staining was performed following standard protocols. Immunostaining was performed on 5-μm-thick paraffin sections using antibodies against phospho-SMAD2 (Thermo Fisher, 44-244G, 1:200), SOX2 (Abcam, ab97959, 1:200), and Cyclin D1 (Abcam, ab134175, 1:200) according to the manufacturer's instructions. For *in situ* hybridization, primers were synthesized and used to amplify cDNA fragments prepared from embryonic mouse incisors. The amplified fragments were cloned into a pGEM®-T Easy vector (Promega), and the resulting plasmids were linearized to serve as templates for probe synthesis. Digoxigenin-labeled riboprobes were transcribed from these templates using T7 or SP6 RNA polymerase (Promega) in the presence of DIG RNA Labeling Mix (Roche). These probes were applied to 12-μm-thick paraffin sections, following standard deparaffinization, rehydration, proteinase K treatment, and hybridization procedures as described previously.[36] Gene expression was visualized by sequential incubation with Anti-DIG-AP Fab fragments (Roche) and BM purple (Roche). Primer sequences are provided in Table S2.

RNA-Seq

Upper incisors were dissected from E14.0 embryos. Total RNA was isolated and subjected to RNA-Seq analysis by BGI (Wuhan, China). For each genotype, two independent samples were sequenced. The genes for which the average FPKM (fragments per kilobase of transcript per million fragments mapped) value was above 1 in WT or *Fst*^{CKO} mice were selected for further analysis. Genes with fold change (FC) $\geq$ 1.5 and Qvalue < 0.001 were considered differentially expressed (Table S1). The advanced volcano plot was generated using OmicStudio tools. Enrichment analysis of RNA-Seq data was performed using Enrichr, which is a comprehensive resource for curated gene sets.[37,38]

Quantitative reverse transcription PCR (qRT-PCR)

qRT-PCR was performed using UltraSYBR mixture (CWBIO, Beijing, China) with the StepOnePlus™ Real-Time PCR System. Upper incisor tooth germs were dissected from E14.0 embryos and total RNA was isolated using Trizol (Thermo Fisher). cDNA was synthesized using RevertAid™ Master Mix (Thermo Fisher, M16325) and used as template in a 20 μl qRT-PCR reaction system. *Actb* was used as a reference gene. To investigate whether *Fst* was successfully deleted in the dental epithelium of *Fst*$^{K14\text{-}Cre}$ mice, cervical loop and ameloblast cells derived from dental epithelium were isolated from the upper incisors of 4-month-old control and *Fst*$^{K14\text{-}Cre}$ mice, and were used for qRT-PCR analysis. To investigate whether *Fst* was deleted in the dental mesenchyme of *Fst*$^{Wnt1\text{-}Cre}$ mice, the dental mesenchyme was isolated from the upper incisors of 4-month-old control and *Fst*$^{Wnt14\text{-}Cre}$ mice and subjected to qRT-PCR. *Gapdh* was used as the reference gene. Primer sequences were from PrimerBank[39] and are shown in Table S2. Data were analyzed using the 2-ΔΔ CT method and are represented as the mean ± SEM. A *p*-value < 0.05 was considered statistically significant.

CUT&Tag

Upper incisors were dissected from E14.0 embryos and subjected to CUT&Tag assays using the Hyperactive In-Situ ChIP Library Prep Kit for Illumina (pA-Tn5) (Vazyme, TD902). Briefly, tooth cells were digested, harvested, mixed with the ConA beads, permeabilized, and incubated with the phospho-SMAD2 antibody or normal rabbit IgG, and the secondary antibody. Subsequently, cells were mixed with the pA-Tn5 Transposon in the tagmentation buffer for targeted tagmentation. DNA was then extracted using phenol/chloroform and precipitated with ethanol, amplified, and used as template for RT-PCR analysis. RT-PCR Primers were designed to amplify the DNA fragments containing

potential p-SMAD2/3-binding sites in the gene regulatory regions (Table S3). Fragments amplified using genomic DNA were used as positive controls for each primer set.

CCK8 assays

Forty-eight hours after transfection with *TBX1* or Scrambled siRNA, HEK293T cells were seeded in DMEM containing 10% FBS at approximately 3000 cells/well into 96-well plates. CCK8 (Sangon, Shanghai, China) solution was added to each well and incubated for 1 h at 37°C. Absorbance at 450 nm was then measured in a microplate reader. The sense sequence of the siRNA for *TBX1* was 5′-GCAAAGAUAGCGAGAAAUA-3′.

Organ culture

Upper incisor tooth germs with some surrounding tissues were dissected from the maxillae of embryos at approximately E14.5 and cultured using a Trowell type organ culture system.[7] Explants were subjected to organ culture and transfected with indicated siRNAs using Lipofectamine® 3000 (Thermo Fisher) on day one. Photographs were taken under light microscopy. The siRNA sense sequences for *Fst* and *Tbx1* were 5′-GGAUGUGAACGACAAUACU-3′ and 5′-UGACCAAUAACCUGCUGGA-3′, respectively. At least six tooth germs were used for each condition in one experiment. The experiments were repeated independently for at least two times.

QUANTIFICATION AND STATISTICAL ANALYSIS

For quantification of proliferation, Cyclin D1-positive cells within a defined area were counted. The intensity of pSMAD2-staining within a defined area was analyzed by the Photoshop Software. Three independent embryonic samples for each genotype were used for statistical analysis. Data was analyzed by GraphPad. Statistical significance was calculated using Student's t-test. A p-value < 0.05 was considered statistically significant.